Pulsed laser deposition of gallium oxide films for high performance solar-blind photodetectors

Fei-Peng Yu,[1] Sin-Liang Ou,[1] and Dong-Sing Wuu[1,2,*]

[1]*Department of Materials Science and Engineering, National Chung Hsing University, Taichung 40227, Taiwan*
[2]*Department of Materials Science and Engineering, Da-Yeh University, Changhua 51591, Taiwan*

[*] *dsw@nchu.edu.tw*

Abstract: Monoclinic gallium oxide thin films were grown on (0001) sapphire at various substrate temperatures ranging from 400 to 1000 °C by pulsed laser deposition using a KrF excimer laser. The structural, optical and compositional properties of the films were analyzed by using x-ray diffraction, transmission electron microscopy, optical transmittance, and Rutherford backscattering spectroscopy. As the substrate temperature was increased to 800 °C, the gallium oxide film possesses single crystalline phase with a preferred growth orientation of (–201) plane and higher crystal quality than those at the other temperatures. Optical transmittance measurements reveal the films grown at 600-1000 °C exhibit a clear absorption edge at the deep ultraviolet region around 250 nm wavelength. Based on the results of Rutherford backscattering spectroscopy, the O/Ga ratio of gallium oxide film increased gradually with increasing substrate temperature. When the substrate temperature was raised to 800-1000 °C, the film composition was close to the formation of Ga_2O_3, indicating the O vacancies and defects were reduced. Furthermore, the films grown at 600 and 800 °C were chosen to fabricate solar-blind metal-semiconductor-metal photodetectors. At an applied bias of 5 V, the photodetector prepared with 800 °C-grown film has a lower dark current of 1.2×10^{-11} A and a higher responsivity of 0.903 A/W (at a wavelength of 250 nm) than those with 600 °C-grown films. The better device performance is ascribed to the higher crystal quality and fewer O vacancies in the 800 °C-grown film. Moreover, the results indicate the gallium oxide films presented in this study have high potential for deep ultraviolet photodetector applications.

©2015 Optical Society of America

OCIS codes: (160.5335) Photosensitive materials; (240.0310) Thin films; (040.7190) Ultraviolet; (230.5160) Photodetectors.

References and links

1. M. Itzler, S. Donati, M. S. Unlu, and K. Kato, "Introduction to the issue on photodetectors and imaging," IEEE J. Sel. Top. Quantum Electron. **10**(4), 665–667 (2004).
2. E. Ozbay, N. Biyikli, I. Kimukin, T. Kartaloglu, T. Tut, and O. Aytur, "High-performance solar-blind photodetectors based on $Al_xGa_{1-x}N$ heterostructures," IEEE J. Sel. Top. Quantum Electron. **10**(4), 742–751 (2004).
3. D. S. Tsai, W. C. Lien, D. H. Lien, K. M. Chen, M. L. Tsai, D. G. Senesky, Y. C. Yu, A. P. Pisano, and J. H. He, "Solar-blind photodetectors for harsh electronics," Sci Rep **3**, 2628 (2013).
4. D. Walker, V. Kumar, K. Mi, P. Sandvik, P. Kung, X. H. Zhang, and M. Razeghi, "Solar-blind AlGaN photodiodes with very low cutoff wavelength," Appl. Phys. Lett. **76**(4), 403–405 (2000).
5. K. W. Liu, D. Z. Shen, C. X. Shan, J. Y. Zhang, D. Y. Jiang, Y. M. Zhao, B. Yao, and D. X. Zhao, "The growth of ZnMgO alloy films for deep ultraviolet detection," J. Phys. D Appl. Phys. **41**(12), 125104 (2008).
6. A. Soltani, H. A. Barkad, M. Mattalah, B. Benbakhti, J. C. De Jaeger, W. J. Zhang, Y. M. Chong, Y. S. Zou, S. T. Lee, A. BenMoussa, B. Giordanengo, and J. F. Hochedez, "193nm deep ultraviolet, visible-blind cBN photodiodes using a new IDTs design based on cubic boron nitride," Appl. Phys. Lett. **92**(5), 053501 (2008).
7. M. Y. Liao, Y. Koide, and J. Alvarez, "Thermally-stable visible-blind diamond photodiode using WC Schottky contact," Appl. Phys. Lett. **87**(2), 022105 (2005).

#233249 - $15.00 USD Received 3 Feb 2015; revised 24 Apr 2015; accepted 24 Apr 2015; published 30 Apr 2015

8. S. P. Arnold, S. M. Prokes, F. K. Perkins, and M. E. Zaghloul, "Design and performance of a simple, room-temperature Ga_2O_3 nanowire gas sensor," Appl. Phys. Lett. **95**(10), 103102 (2009).
9. R. Zou, Z. Zhang, Q. Liu, J. Hu, L. Sang, M. Liao, and W. Zhang, "High detectivity solar-blind high-temperature deep-ultraviolet photodetector based on multi-layered (l00) facet-oriented β-Ga_2O_3 nanobelts," Small **10**(9), 1848–1856 (2014).
10. Y. Kokubun, K. Miura, F. Endo, and S. Nakagomi, "Sol-gel prepared β-Ga_2O_3 thin films for ultraviolet photodetectors," Appl. Phys. Lett. **90**(3), 031912 (2007).
11. T. Oshima, T. Okuno, N. Arai, N. Suzuki, S. Ohira, and S. Fujita, "Vertical solar-blind deep-ultraviolet Schottky photodetectors based on beta-Ga_2O_3 substrate," Appl. Phys. Express **1**(1), 011202 (2008).
12. W. Y. Weng, T. J. Hsueh, S. J. Chang, G. J. Huang, and H. T. Hsueh, "A β-Ga_2O_3 Solar-Blind Photodetector Prepared by Furnace Oxidization of GaN Thin Film," IEEE Sens. J. **11**(4), 999–1003 (2011).
13. T. Oshima, T. Okuno, and S. Fujita, "Ga_2O_3 Thin Film Growth on *c*-Plane Sapphire Substrates by Molecular Beam Epitaxy for Deep-Ultraviolet Photodetectors," Jpn. J. Appl. Phys. **46**(11), 7217–7220 (2007).
14. D. Y. Guo, Z. P. Wu, Y. H. An, X. C. Guo, X. L. Chu, C. L. Sun, L. H. Li, P. G. Li, and W. H. Tang, "Oxygen vacancy tuned Ohmic-Schottky conversion for enhanced performance in β-Ga_2O_3 solar-blind ultraviolet photodetectors," Appl. Phys. Lett. **105**(2), 023507 (2014).
15. D. Guo, Z. Wu, P. Li, Y. An, H. Liu, X. Guo, H. Yan, G. Wang, C. Sun, L. Li, and W. Tang, "Fabrication of β-Ga_2O_3 thin films and solar-blind photodetectors by laser MBE technology," Opt. Mater. Express **4**(5), 1067–1076 (2014).
16. P. Ravadgar, R. H. Horng, S. D. Yao, H. Y. Lee, B. R. Wu, S. L. Ou, and L. W. Tu, "Effects of crystallinity and point defects on optoelectronic applications of β-Ga_2O_3 epilayers," Opt. Express **21**(21), 24599–24610 (2013).
17. T. C. Wei, D. S. Tsai, P. Ravadgar, J. J. Ke, M. L. Tsai, D. H. Lien, C. Y. Huang, R. H. Horng, and J. H. He, "See-Through Ga_2O_3 Solar-Blind Photodetectors for Use in Harsh Environments," IEEE J. Sel. Top. Quantum Electron. **20**(6), 3802006 (2014).
18. T. Y. Tsai, R. H. Horng, D. S. Wuu, S. L. Ou, M. T. Hung, and H. H. Hsueh, "GaN Epilayer Grown on Ga_2O_3 Sacrificial Layer for Chemical Lift-Off Application," Electrochem. Solid-State Lett. **14**(11), H434–H437 (2011).
19. L. Guo, X. Shen, G. Zhu, and K. Chen, "Preparation and gas-sensing performance of In_2O_3 porous nanoplatelets," Sens. Actuators B Chem. **155**(2), 752–758 (2011).
20. S. S. Kumar, E. J. Rubio, M. Noor-A-Alam, G. Martinez, S. Manandhar, V. Shutthanandan, S. Thevuthasan, and C. V. Ramana, "Structure, morphology, and optical properties of amorphous and nanocrystalline gallium oxide thin films," J. Phys. Chem. C **117**(8), 4194–4200 (2013).
21. Z. L. Wang, J. S. Yin, and Y. D. Jiang, "EELS analysis of cation valence states and oxygen vacancies in magnetic oxides," Micron **31**(5), 571–580 (2000).
22. A. Linsebigler, G. Lu, and J. T. Yates, "CO chemisorption on TiO_2(110): Oxygen vacancy site influence on CO adsorption," J. Chem. Phys. **103**(21), 9438–9443 (1995).
23. J. A. Garrido, E. Monroy, I. Izpura, and E. Munoz, "Photoconductive gain modelling of GaN photoconductors," Semicond. Sci. Technol. **13**(6), 563–568 (1998).

1. Introduction

Recently, photodetector (PD) devices have been extensively investigated owing to their large number of applications including flame detection, tracking missiles, photolithography, automatization, intersatellite communication, biochemicals, and so on [1–3]. In particular, deep ultraviolet (DUV) PDs with solar-blind sensitivity (cut-off wavelength shorter than 280 nm) have attracted a strong interest since their photoresponse can be further constrained in the DUV region even at sun or room illuminations [1]. Up to now, lots of materials have been developed for the PD applications. Between these materials, several wide band gap semiconductors, such as AlGaN, ZnMgO, BN, and diamond possess high potential for the fabrication of solar-blind DUV detectors [4–7]. However, as the AlGaN PD is prepared, the device performance easily tends to degrade with increasing Al concentration. For the ZnMgO growth, it is very difficult to maintain its single wurtzite structure due to the phase segregation of rock salt MgO as the band gap is larger than 4.5 eV. The major drawbacks of BN and diamond PDs are their large band gaps of 6.3 and 5.5 eV, which cause the sensitivity ranges to be limited to cut-off wavelengths shorter than 193 and 225 nm, respectively.

Monoclinic gallium oxide (β phase) is the other material with large cut-off wavelength (250–280 nm), which leads to detection over the full range of DUV [8]. In addition, gallium oxide possesses high chemical and thermal stability [9]. Thus, compared with these materials mentioned above, monoclinic gallium oxide is more suitable for the fabrication of DUV PDs. In recent years, nanostructure, thin-film, and bulk gallium oxide solar-blind PDs have been proposed [9–11]. For practical purposes, thin-film type PDs are the most popular form for

device fabrication. For the thin-film type gallium oxide PDs, several techniques have been used to deposit the films, such as sol-gel methods [10], furnace oxidization of GaN [12], molecular beam epitaxy (MBE) [13], laser MBE [14, 15], and metalorganic chemical vapor deposition (MOCVD) [16, 17]. For the thin-film type gallium oxide PD, the crystal quality of the film would affect the device performance significantly. However, gallium oxide films with single crystalline structure are very hard to grow. Recently, our research group has proposed single crystalline gallium oxide films with high crystal quality by MOCVD, and the device performance of solar-blind PD is obviously improved [16]. It is well known that the MOCVD system is mainly employed to grow nitride-based materials. For the growth of oxide-based materials, the MOCVD system should be modified, which would increase the fabrication cost of PD devices and lower feasibility of mass production. As a result, another growth technology for the single crystalline gallium oxide film is required.

Based on our previous research, single crystalline β-Ga_2O_3 thin films have also been prepared by pulsed laser deposition (PLD) and used as a sacrificial layer for chemical lift-off application [18]. For the thin film growth, PLD is an ideal technique since the atomic-layer control can be realized by adjusting the laser repetition rate and the source particles possess high energy which enhances the surface mobility of the ad-atoms. At present, the solar-blind PD containing the gallium oxide thin film fabricated by PLD has seldom been investigated. In this study, 220-nm-thick gallium oxide films were prepared by PLD with various substrate temperatures from 400 to 1000 °C. Furthermore, the gallium oxide films were employed to fabricate the solar-blind PDs. The structural, optical, and compositional characteristics of gallium oxide films and device performance of PDs were analyzed in detail.

2. Experimental

In this study, gallium oxide films were prepared on c-plane sapphire substrates with a diameter of 2 inch by using PLD (PLD/MBE-2000, PVD products). A stoichiometric ceramic Ga_2O_3 target (99.99% purity) with 7.62 cm diameter was employed for the gallium oxide deposition. The distance between the Ga_2O_3 target and sapphire substrate was fixed at 50 mm. During the film's growth, the substrate temperatures of 400, 600, 800, and 1000 °C were chosen. A KrF excimer laser (λ = 248 nm) was used as an ablation source, and its repetition rate and pulse energy density were fixed at 10 Hz and 2.4 J/cm^2, respectively. When the deposition chamber was pumped to a base pressure below 2×10^{-9} Torr, oxygen gas (99.999%) was introduced into the chamber, and the working pressure was kept at 2×10^{-1} Torr. The thickness of the gallium oxide film was 220 nm. The crystal structure and quality of the films were investigated by x-ray diffraction (XRD) (PANalytical, X'Pert Pro MRD). Cu K_α radiation (λ = 1.5418 Å) was used as the source and Ge (220) was employed as the monochromator for XRD. The transmittance spectra of the gallium oxide films were analyzed by the N&K analyzer (model: 1280, N and K Tech.) with wavelengths ranging from 200 to 800 nm. The cross-sectional image of the sample was observed by scanning electron microscopy (SEM). The microstructure of the film was characterized by high-resolution transmission electron microscopy (HR-TEM, model: JEM-2100 F). The compositions of the films were determined by Rutherford backscattering spectroscopy (RBS). Rump software was adopted to simulate and transact the RBS data.

In the device process of the solar-blind metal-semiconductor-metal (MSM) PD, a Ni/Au (50/100 nm) film grown onto the sample by thermal evaporation was adopted as the Schottky contact metal. By using standard photolithography and wet etching processes, the interdigitated contact electrodes can be prepared. Figure 1 exhibits a schematic diagram of the fabricated PD device. We can observe that the size of interdigitated pattern on the shadow mask was 2000 μm wide and 2200 μm long. Moreover, the finger width and interspacing were both 100 μm. After fabricating the device, several performance characteristics were analyzed. Current–voltage (I-V) characteristics of the solar-blind MSM PDs were measured by a HP 4156 semiconductor analyzer at room temperature in dark environment. Spectral

responsivity measurements were carried out by using a Jobin-Yvon Spex system with a 300 W xenon arc lamp light source (Perkin-Elmer PE300BUV) and a standard synchronous detection scheme measured at the frequency of 300 Hz. Time-dependent photoresponsivity was performed at a constant voltage of 5 V.

It should be mentioned that eight films were prepared at each temperature. Moreover, for the fabrication of MSM PDs, the 600 °C- and 800 °C-grown gallium oxide films were used, and ten devices were prepared at each condition. The characteristics of gallium oxide films and the device performance of MSM PDs were similar to each other when the same fabrication condition was used. This indicates that the PLD technique and the device process presented in our work both possess high fabrication stability. In this research, the results were all representative data from multiple samples.

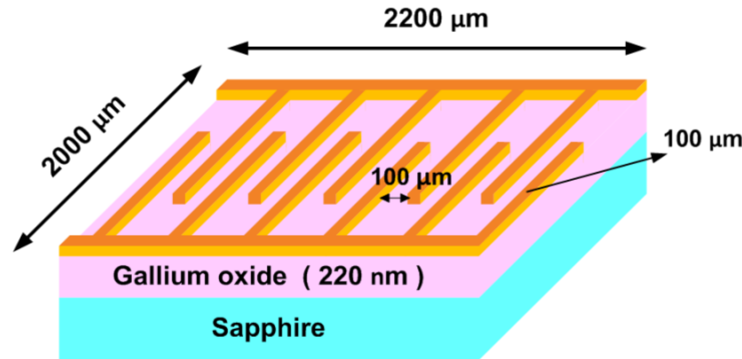

Fig. 1. Schematic diagram of the fabricated gallium oxide MSM PD.

3. Results and discussion

Figure 2(a) displays the XRD patterns of the gallium oxide films grown at various substrate temperatures. When the substrate temperature was heated to 400 °C, only a Al_2O_3 (0006) diffraction peak can be detected in the film, which was attributed to the crystalline nature of the sapphire substrate. No diffraction peak indexed to Ga_2O_3 or other phase formed in the 400 °C-grown film, which revealed that the crystal structure of this film was amorphous. The formation of amorphous structure can be ascribed to low surface migration of ad-atoms, which would restrict the growth of the crystalline phase in the crystallization process. Further increasing the substrate temperature to 600 and 800 °C, the XRD patterns presented three peaks indexed to (–201), (–402), and (–603) planes both within these two gallium oxide films. These three peaks belonging to the (–201) plane family were associated to the β-Ga_2O_3 phase. On the other hand, the XRD patterns also implied that the 600 °C- and 800 °C-grown gallium oxide films both possessed single crystalline structure. With increasing substrate temperature from 600 to 800 °C, the intensities of these diffraction peaks belonging to the β-Ga_2O_3 (–201) plane family all increased. This phenomenon can be explained by the thermal energy supplied from the substrate temperature. Compared with the 600 °C-grown film, more thermal energy can be provided to the ad-atoms on the substrate while the substrate temperature was increased to 800 °C, leading to improvements in the surface mobility and the intensity of (–201) plane family orientation. As the sapphire substrate was heated to 1000 °C during the growth process, the peaks of (–201) plane family still existed in the XRD pattern. However, the other diffraction peaks indexed to (400) and (–801) planes of β-Ga_2O_3 phase were also generated in the 1000 °C-grown film, indicating that this film had a polycrystalline nature. Owing to the high substrate temperature of 1000 °C for the film growth, the arrangement of atoms in the gallium oxide film could be destroyed, inducing the formation of polycrystalline structure. Figure 2(b) shows the XRD rocking curves of (–201) diffraction peak for the gallium oxide films deposited at the substrate temperatures of 600, 800, and 1000 °C. For the

#233249 - $15.00 USD Received 3 Feb 2015; revised 24 Apr 2015; accepted 24 Apr 2015; published 30 Apr 2015

film prepared at 600 °C, the full width at half maximum (FWHM) value of rocking curve at (–201) plane was determined to be 516 arcsec. When the substrate temperature was increased to 800 and 1000 °C, the FWHM values of (–201) plane were reduced to 359 and 402 arcsec, respectively. It is obvious that the 800 °C-grown film possesses higher crystal quality than the others.

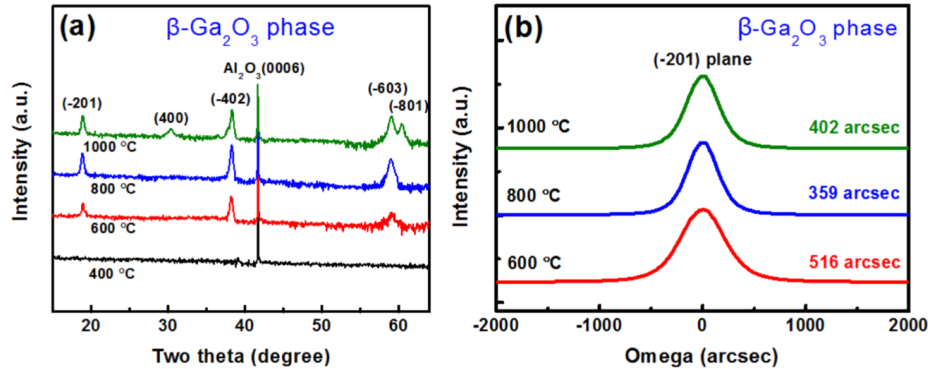

Fig. 2. (a) XRD patterns of the gallium oxide films grown at various substrate temperatures (400–1000 °C) and (b) XRD rocking curves for (–201) plane of the films grown at 600, 800, and 1000 °C.

Figure 3 displays the transmittance spectra of the gallium oxide films prepared at various substrate temperatures of 400–1000 °C. It can be observed that the films deposited at 600, 800, and 1000 °C show an obvious absorption edge at the DUV region near a wavelength of 250 nm. The sharp absorption occurring at the band edge proves that the gallium oxide films grown at 600–1000 °C possess crystalline nature. The result is in good agreement with the XRD patterns, as shown in Fig. 2(a). Additionally, the feature of transmittance for the gallium oxide film grown at 400 °C was much different than that of the other films. The 400 °C-grown film possessed a transmittance spectrum with a smooth but not sharp absorption edge near 270–285 nm and relatively lower transmittance (<30%) in the measured wavelength range. This is owing to the amorphous structure within the 400 °C-grown film. Because the gallium oxide material has a direct band gap, its absorption coefficient (α) can be evaluated by using the following equation [19, 20]:

$$\alpha h\nu = C(h\nu - E_g)^{1/2}$$

where C is a constant, v is the frequency of the incident photon, h is Planck's constant, and E_g is the optical band gap of the thin film. After extrapolating the linear region near the onset in a plot of α^2 versus $h\nu$, the optical band gap can be estimated. Then the E_g values of the gallium oxide films deposited at 400, 600, 800, and 1000 °C were determined to be 4.65, 4.86, 4.92, and 4.96 eV, respectively. The absorption edge of the gallium oxide films shifted towards the short wavelength region gradually (blue shift) with increasing substrate temperature. Besides, the result also indicates that the PLD-deposited gallium oxide films are highly suitable for DUV light detection.

Then we used the RBS measurement to analyze the atomic compositions of these gallium oxide films. In these films, the atomic composition changes when the substrate temperature varies, as shown in Table 1. The O/Ga ratios of these four films grown at 400, 600, 800, and 1000 °C were determined to be 1.17, 1.29, 1.46, and 1.48, respectively. Apparently, the O/Ga ratio increases with increasing substrate temperature, which indicates that the composition of gallium oxide film is close to the formation of Ga_2O_3, especially for the samples prepared at the substrate temperatures of 800 and 1000 °C. It can be estimated that relatively fewer net vacancies or interstitials (point defects) formed in the 800 °C- and 1000 °C-grown films, as

#233249 - $15.00 USD Received 3 Feb 2015; revised 24 Apr 2015; accepted 24 Apr 2015; published 30 Apr 2015

compared with the films deposited at 400 and 600 °C. Based on previous research, Ga vacancies and O interstitials play the roles of effective positive ions (cations); meanwhile, O vacancies and Ga interstitials behave as effective negative ions (anions) [21, 22]. The formation of O vacancies, Ga vacancies, and O-Ga vacancy pairs would be responsible for the defects of the gallium oxide film.

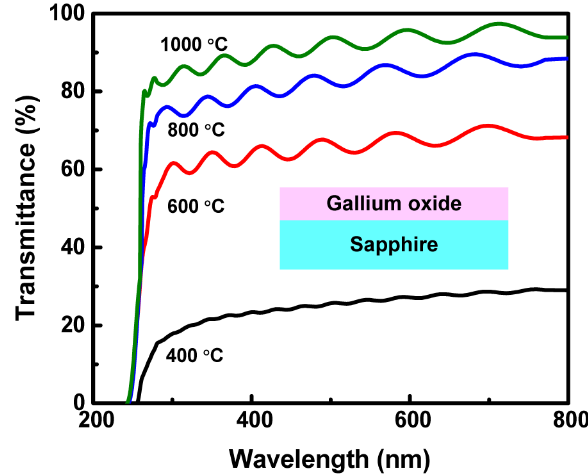

Fig. 3. Transmittance spectra of the gallium oxide films grown at 400–1000 °C.

Table 1. Atomic compositions of PLD-deposited gallium oxide films on sapphire substrates under various substrate temperatures measured by Rutherford backscattering spectroscopy.

Substrate temperature	Ga (%)	O (%)	O/Ga
400 °C	46.08	53.92	1.17
600 °C	43.67	56.33	1.29
800 °C	40.65	59.35	1.46
1000 °C	40.32	59.68	1.48

Figure 4(a) shows the cross-sectional SEM image of 800 °C-grown gallium oxide film on sapphire substrate, where the interface between the film and substrate can be clearly identified. Additionally, the HR-TEM bright field images of gallium oxide films deposited at 800 and 1000 °C are displayed in Figs. 4(b) and 4(c), respectively. These TEM images indicate good crystallinity in the films. Moreover, the d-spacings of the films prepared at 800 and 1000 °C were evaluated to be 4.62 and 4.65 Å, respectively, which corresponded to the β-Ga_2O_3 (–201) plane based on the JCPDs card. Because of the similar oxygen atom arrangements on a c-plane sapphire substrate and a β-Ga_2O_3 (–201) plane, the gallium oxide films mainly consisted of (–201)-oriented planes [13]. On the other hand, within the 1000 °C-grown film, the other d-spacing of 1.52 Å indexed to β-Ga_2O_3 (–801) plane was also found, which agreed well with the XRD result, as shown in Fig. 2(a).

As mentioned above, the gallium oxide film with single crystalline β-Ga_2O_3 phase can result in better device performance as the MSM PD was fabricated. Therefore, based on the XRD result, we chose the 600 °C- and 800 °C-grown gallium oxide films to prepare MSM PDs and investigate their device performances. Although these two films both possessed single crystalline β-Ga_2O_3 phase, the crystal quality and O/Ga ratio are much different between them. The room temperature I–V curves characterized in dark environment of these two PDs are shown in Fig. 5. The inset in Fig. 5 is the cross-sectional schematic diagram of the detector device. It can be observed that the dark current of the PD fabricated with 800 °C-grown gallium oxide film was obviously smaller than that with 600 °C-grown film. Under the

same bias voltage, there is a large difference in dark current of approximately 1–2 orders of magnitude between these two MSM PDs. The result indicated that a high leakage current existed in the PD fabricated with 600 °C-grown film, which was attributed to more oxygen vacancies and poor crystal quality. The oxygen vacancies in the gallium oxide film would result in many free electrons from gallium atoms. When the substrate temperature was increased to 800 °C, the crystal quality of the gallium oxide film in comparison to that deposited at 600 °C was obviously enhanced, as shown in Fig. 2(b). In addition, from the RBS result, the O/Ga ratio of the gallium oxide film increased from 1.29 to 1.46 with an increment of substrate temperature from 600 to 800 °C, which led to much fewer oxygen vacancies formed in the film grown at 800 °C. As a result, the 800 °C-grown film had lower leakage current than that of 600 °C-grown film. With an applied bias of 5 V, the measured dark currents of these two devices fabricated with 600 °C- and 800 °C-grown gallium oxide films were 3.9×10^{-10} and 1.2×10^{-11} A, respectively. Moreover, the small dark currents can be ascribed to the highly resistive nature of the β-Ga_2O_3 crystalline phase.

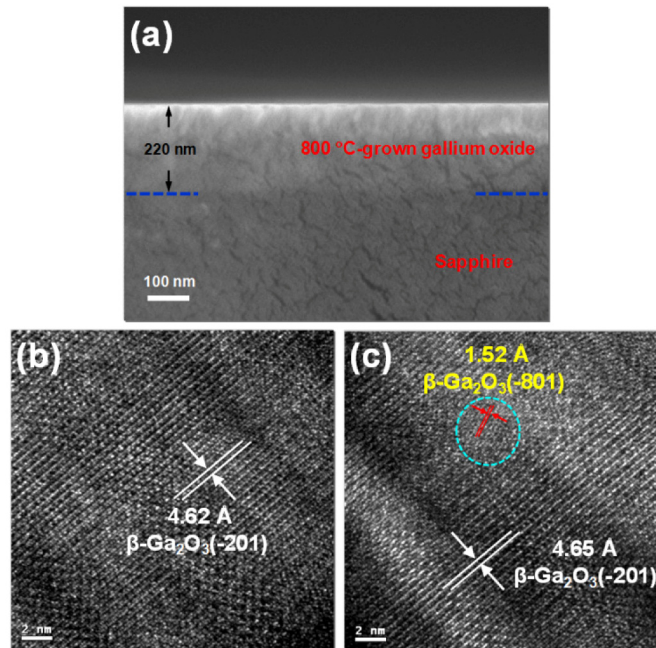

Fig. 4. (a) Cross-sectional SEM image of the 800 °C-grown gallium oxide film on sapphire substrate and HR-TEM bright field images of the films grown at (b) 800 and (c) 1000 °C.

#233249 - $15.00 USD Received 3 Feb 2015; revised 24 Apr 2015; accepted 24 Apr 2015; published 30 Apr 2015

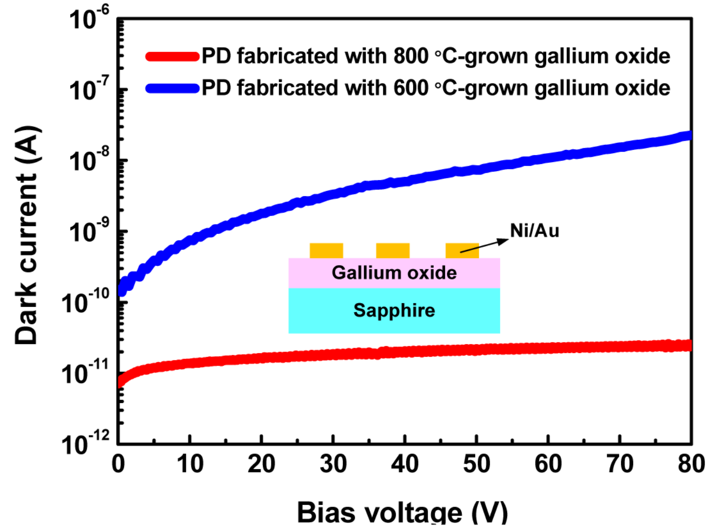

Fig. 5. Current-voltage characteristics measured in dark for the PDs fabricated with 600 °C- and 800 °C-grown gallium oxide films. The inset is the cross-sectional schematic diagram of the PD device.

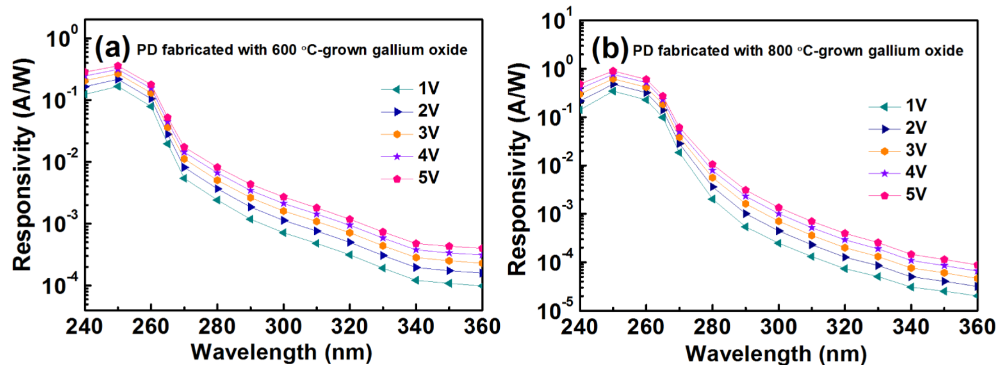

Fig. 6. Spectral responsivities of the DUV detectors based on (a) 600 °C- and (b) 800 °C-grown gallium oxide films.

Figures 6(a) and 6(b) exhibit the responsivities as a function of wavelength for the MSM PDs fabricated with 600 °C- and 800 °C-grown gallium oxide films, where the measurements were biased at 1–5 V. The light was incident on the front side of the device as the measurement was performed. In this measurement, the wavelength was increased from 240 to 360 nm. It can be seen that these two devices both exhibited a maximum responsivity around 250 nm, which confirmed that the gallium oxide PDs were really solar-blind. In addition, the drop at 250 nm is in good agreement with the optical band gap of 4.8–5.0 eV of these two films. Compared with these two devices, we can observe that the cut-off wavelength of the device fabricated with 800 °C-grown film was more obvious than that with 600 °C-grown film. Under a bias voltage of 5 V, the peak responsivity of the device with 600 °C-grown film was 0.359 A/W, and its DUV-to-visible discrimination ratio (the contrast ratio between 250 and 350 nm) was 833. Meanwhile, when the MSM PD was prepared with 800 °C-grown film, its peak responsivity (@5 V) and DUV-to-visible discrimination ratio were 0.903 A/W and 7867, respectively. The higher responsivity and larger DUV-to-visible discrimination ratio of the latter device can be attributed to the better crystal quality and fewer O vacancies in the 800 °C-grown film. Furthermore, these two devices both exhibited increasing responsivity

#233249 - $15.00 USD Received 3 Feb 2015; revised 24 Apr 2015; accepted 24 Apr 2015; published 30 Apr 2015

with increasing bias voltage, which suggested that the devices had large photoconductive gain [23].

Figure 7 shows a time-dependent response of the MSM PD fabricated with the 800 °C-grown gallium oxide film biased at 5 V as the 254 nm exciting light was switched on and off. According to the measured result, the dark current was around of 1×10^{-11} A, which was very low and useful in PD applications. Under 254 nm illumination, the current increased instantaneously to a stable value of approximately 1.8×10^{-6} A. We can find that the dynamic response of the MSM PD was stable and reproducible, where the on/off current contrast ratio was about 10^5. Moreover, it was also observed that the increment of photocurrent was rapid when the exciting light was turned on. However, by turning off the exciting light, a relatively slow response occurred in the device. This slight decay in response was probably ascribed to the oxygen-related hole-trap states generated at the surface of gallium oxide film [12]. These hole-trap states would reduce charge carrier recombination because some carriers are captured as the traps empty. Therefore, a slightly longer tail in the photoresponse occurred when the exciting light was turned off (Fig. 7). Additionally, the rise time (from 10% to 90% of maximum photocurrent) and fall time (from 90% to 10% of maximum photocurrent) of the photoresponse shown in Fig. 7 were smaller than 1 and 3 sec, respectively.

A summary of the solar-blind MSM PDs fabricated with the gallium oxide films grown by various techniques is shown in Table 2. These films were deposited by sol-gel method, furnace oxidization of GaN, MBE, laser MBE, MOCVD, and PLD (this study). In these techniques, the high preparation temperatures (such as growth, annealing, and oxidization temperatures) of 700-1000 °C for gallium oxide films are required. In addition, the high temperature would not affect the fabrication of thin-film solar-blind MSM PDs because the device process is performed after preparing the gallium oxide film. The crystalline states of gallium oxide films and device performances of PDs are compared. It can be seen that single crystalline gallium oxide films can be obtained by using MBE, laser MBE, MOCVD, and PLD. The performance of the MSM PD fabricated by sol-gel method is relatively low, probably resulting from the poor crystal quality of gallium oxide film. Obviously, the device with the gallium oxide film prepared by laser MBE has better performance than that prepared by MBE. When the MOCVD technique is used to grow the gallium oxide film, the fabricated MSM PD possesses an extremely low dark current. However, as mentioned above, the cost issue of modified MOCVD system should be considered. In our work, the solar-blind detector containing the gallium oxide film grown by PLD shows good device characteristics. Actually, the improvement in the performance of this PD can be continued by optimizing some fabrication parameters including the spacing of the electrodes and the interface of the metal-electrode/semiconductor.

The diameter of sapphire substrates used in this study for the growth of gallium oxide films by PLD is 2 inch. This reveals that gallium oxide films with single crystalline structure grown on 2-inch-diameter sapphire substrates can be obtained in our work. Moreover, 220-nm-thick gallium oxide films prepared by PLD can exhibit high thickness uniformity as good as those by MOCVD. In fact, for commercial applications in the optoelectronic devices, the diameter of the sapphire substrate is usually larger than 4 inch, and this is commonly used for MOCVD growth. However, the substrate with a larger diameter than 4 inch has seldom been employed as the film is grown by PLD, and the PLD-deposited film on this substrate could deteriorate the thickness uniformity. In the future, the PLD equipment may be further designed to apply for the film's growth on the substrate with a larger diameter, and it will possess high feasibility for commercial applications.

#233249 - $15.00 USD Received 3 Feb 2015; revised 24 Apr 2015; accepted 24 Apr 2015; published 30 Apr 2015

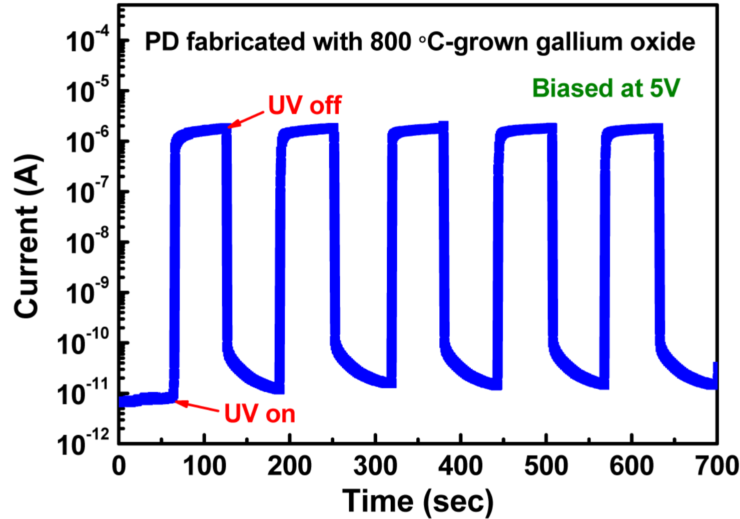

Fig. 7. Transient response of the PD device fabricated with 800 °C-grown gallium oxide film.

Table 2. Summary of the solar-blind MSM PDs fabricated with the gallium oxide films grown by various techniques. The crystalline states of gallium oxide films and device performances of PDs are compared.

Deposition method	Crystalline state of gallium oxide	device performance	Reference
Sol-gel method	Polycrystalline	Max. responsivity (@10 V): 8×10^{-5} A/W	10
Furnace oxidization of GaN	Polycrystalline	Max. responsivity (@5 V): 0.453 A/W Dark current (@5 V): 1.39×10^{-10} A	12
MBE	Single crystalline	Max. responsivity (@10 V): 0.037 A/W Dark current (@10 V): 1.4×10^{-9} A	13
Laser MBE	Single crystalline	Dark current (@1 V): 3.1×10^{-10} A	14
MOCVD	Single crystalline	Dark current (@5 V): 4×10^{-12} A	16
PLD	Single crystalline	Max. responsivity (@5 V): 0.903 A/W Dark current (@5 V): 1.2×10^{-11} A	This study

4. Conclusions

Gallium oxide films were deposited on sapphire substrates at various temperatures from 400 to 1000 °C in oxygen ambient by PLD. With increasing substrate temperature, the structure of gallium oxide film varied from amorphous to β-Ga_2O_3 crystalline phase. At a substrate temperature of 800 °C, the single crystalline gallium oxide film has higher crystal quality than that of the others. Compositional analyses reveal the O/Ga ratio of the gallium oxide film increases with increasing substrate temperature. Especially for the substrate temperatures of 800–1000 °C, the film composition was close to the stoichiometric Ga_2O_3. Additionally, the 600 °C- and 800 °C-grown films were selected to prepare the solar-blind MSM PDs. As a 5-V bias is applied, the device fabricated with 800 °C-grown film possesses better performance, where its dark current and responsivity are 1.2×10^{-11} A and 0.903 A/W (at a wavelength of 250 nm), respectively. This can be owing to the higher crystal quality and fewer O vacancies existing in the 800 °C-grown film. Obviously, the PLD-deposited gallium oxide films show high potential in DUV detector applications.

Acknowledgments

This work was supported by the Ministry of Economic Affairs (Taiwan, R.O.C.) under Grant No. 102-E0605 and National Science Council (Taiwan, R.O.C.) under the Contract Nos. 102-2221-E-005-072-MY3 and 102-2811-E-005-004.